Experimental and Computational Fluid Dynamics Investigation on Tanning Process in a Rotating Drum

by

Yirui Lin,[1] Zhuocheng Jiang,[2] Ya-nan Wang,[1,3] Yunhang Zeng,[1,3]* Guo Xie[2]*and Bi Shi[1,3]

[1]*National Engineering Laboratory for Clean Technology of Leather Manufacture, Sichuan University,* Chengdu 610065, China

[2]*State Key Laboratory of Hydraulics and Mountain River Engineering, College of Water Resource & Hydropower,* Sichuan University, Chengdu 610065, China

[3]*Key Laboratory of Leather Chemistry and Engineering (Sichuan University), Ministry of Education,* Chengdu 610065, China

Abstract

Mass transfer of chemicals greatly affects leather production efficiency and product quality. Leather shows different motions in a rotating drum during processing, which is strongly associated with chemicals' mass transfer. However, how leather motions affect mass transfer remains unclear, which disfavors highly efficient leather manufacturing process. Here, different leather motion states were obtained by adjusting the drum rotation speed. Experimental results showed that the duration of leather rolling motion greatly increased by 41% when the rotation speed increased from 5 r/min to 20 r/min, and the uptake of the tanning agent was consequently improved, which indicated that the rolling motion is beneficial to mass transfer. Computational fluid dynamics simulation results showed that the mass transfer rate under rolling motion was higher than those under slipping, elevating and hanging motions, because the flow velocity and concentration gradient near the leather surface were higher under rolling motion. Accordingly, increasing the rolling motion enhanced the mass transfer in leather processing. This work identifies the leather motion beneficial for mass transfer and provides guidance on operating condition optimization and drum design for high-efficiency leather production.

Introduction

Leather manufacturing converts animal hides/skins, the by-products of the meat industry, into valuable leather products, which offers important economic benefits and reduces the waste of natural resources.[1] The leather making process is divided into four stages: beamhouse, tanning, post-tanning and finishing.[2] In the first three stages, hides/skins are processed in a rotating drum with various chemicals, involving surfactant, sodium sulfide, lime, ammonium sulphate, enzyme, acid, basic chromium sulphate, acrylic resin, vegetable tannin, and dyestuff [Figure 1(a)].[3] These chemicals react with hide collagen fibers which are the vital components of leather and endow the leather with satisfactory properties (i.e. hydrothermal stability, resistance to bacteria/enzymes, flexibility, comfortable feel, beautiful colors).[4] However, the transfer of chemicals into hides/skins is greatly resisted by the complicated porous fiber network of hides/skins.[5,6] Further, the chemicals are prone to combine with collagen fibers on the hide surface through covalent bonding, coordination, electrostatic interaction, hydrogen bonding, van der Waals interaction or hydrophobic interaction, which negatively affects the transfer of chemicals to the inner hide [Figure 1(a)].[7] Rapid penetration and uniform distribution of chemicals in leather play an important role in the quality and production efficiency of leather. For example, tanning agents that can make hides resistant to thermal shrinkage and bacteria/enzymes are considered the most important chemicals for leather making. However, they are easily deposited on the hide surface through chemical interactions, which leads to the rough surface and low hydrothermal stability of leather. Therefore, the mass transfer enhancement of chemicals has received much attention for producing high-quality leather.

Extensive research has shown that the most important factors influencing the solid–liquid mass transfer process are interfacial turbulence,[8-10] two-phase contact area,[11] the diffusion rate of components[12] and the properties of solids and liquids.[13,14] In the leather industry, many attempts have been made to enhance the mass transfer of chemicals in hides/skins, such as adjusting the surface charge of hides/skins,[15-17] the properties of chemicals (charge, functional groups and molecular weights)[18-21] and the amount or properties of liquid (dielectric constant, density and chemical bond)[22,23] in the drum. These attempts show promising potential for the rapid penetration and high uptake of chemicals. Notably, the mechanical actions of the drum (rolling, collision, extrusion and pulling) also greatly affect the mass transfer of chemicals in leather. In fact, tanners have found that optimizing the operating conditions (rotation speed, loading quantity, the ratio of leather to float) and drum structure is an efficient way to improve the mass transfer of chemicals and is even superior to the above methods.[24-26] However, the operating drum conditions are often determined by the experience of tanners rather than scientific theory. In the rotating drum, the leather shows various motion characteristics, including velocities and motion states [Figure 1(b)], which bring about the variation of interfacial turbulence and

*Corresponding authors email: zengyunhang@scu.edu.cn (Y . H. Zeng), 2008xieguo@scu.edu.cn (G. Xie)

Manuscript received April 17, 2023, accepted for publication June 25, 2023.

the contact area between leather and float. Previous studies have focused on the chemical reactions between leather and chemicals, but little attention has been paid to how to optimize the drum mechanical actions and the motion characteristics of leather. Hence, the quantitative relationship between leather motion characteristics and the mass transfer of chemicals remains unclear. Undoubtedly, this knowledge gap hinders scientific guidance in the adjustment of drum mechanical actions and the mass transfer enhancement of leather chemicals.

Computational fluid dynamics (CFD) simulation is a powerful method for investigating the mass transfer process in a rotating flow field. Santos et al. studied the particle dynamic behavior in a rotating drum by CFD method and obtained the different solid flows and velocity distributions of the particulate phase.[27] Shi et al. performed a CFD method to analyze the liquid-phase flow within rotating packed bed (RPB) reactors and obtained the velocity and distribution of the liquid in RPB and the interface between gas–liquid phases.[28] Tang et al. used the CFD method to investigate a mixing process in a solid–liquid rotary drum and determine the effect of rotation speed on particle behaviors and flow characteristics.[29]

Therefore, in the present work, an attempt was made to quantitatively clarify the influence of typical leather motions on chemicals' mass transfer in leather by experimental and CFD simulation methods. Different leather motions were prepared by adjusting the drum rotation speed, as described in a previous work.[30] Pickled cattle hides were tanned with an environmentally friendly zirconium tanning agent under the different leather motions. Then, the adsorption kinetics of the tanning agent and the tanning performance of leather were analyzed to determine the relationship between leather motions and chemicals' transfer and reaction. Moreover, the velocity distributions of flow field and the mass transfer rates of the zirconium tanning agent under each typical motion state were investigated by CFD simulation based on the experimental data [Figure 1(c)] to further explain how leather motion states affect the mass transfer rate of chemicals. Here, it is worth noting that although the chrome tanning method is the most common tannage used in the leather industry, it generates chromium-containing wastewaters and solid wastes.[31,32] Therefore, chrome-free tannages have received much attention in recent years.[33] Zirconium tanning is a typical chrome-free tannage, and zirconium is easily detected by energy-dispersive X-ray spectroscopy (EDS) and inductively coupled plasma optical emission spectrometry (ICP-OES).[34] Moreover, the transfer rate and distribution uniformity of the zirconium tanning agent in the hide are inferior to those of the chrome tanning agent,[35] and thus the difference in the tanning performance under various rotation speeds can be observed more easily during zirconium tanning. For these reasons, zirconium tanning was chosen to investigate the tanning process in this work. This study is expected to identify the leather motion state that is more beneficial for chemicals' mass transfer and provide basic guidance on the optimization of operating conditions and the design of novel drum.

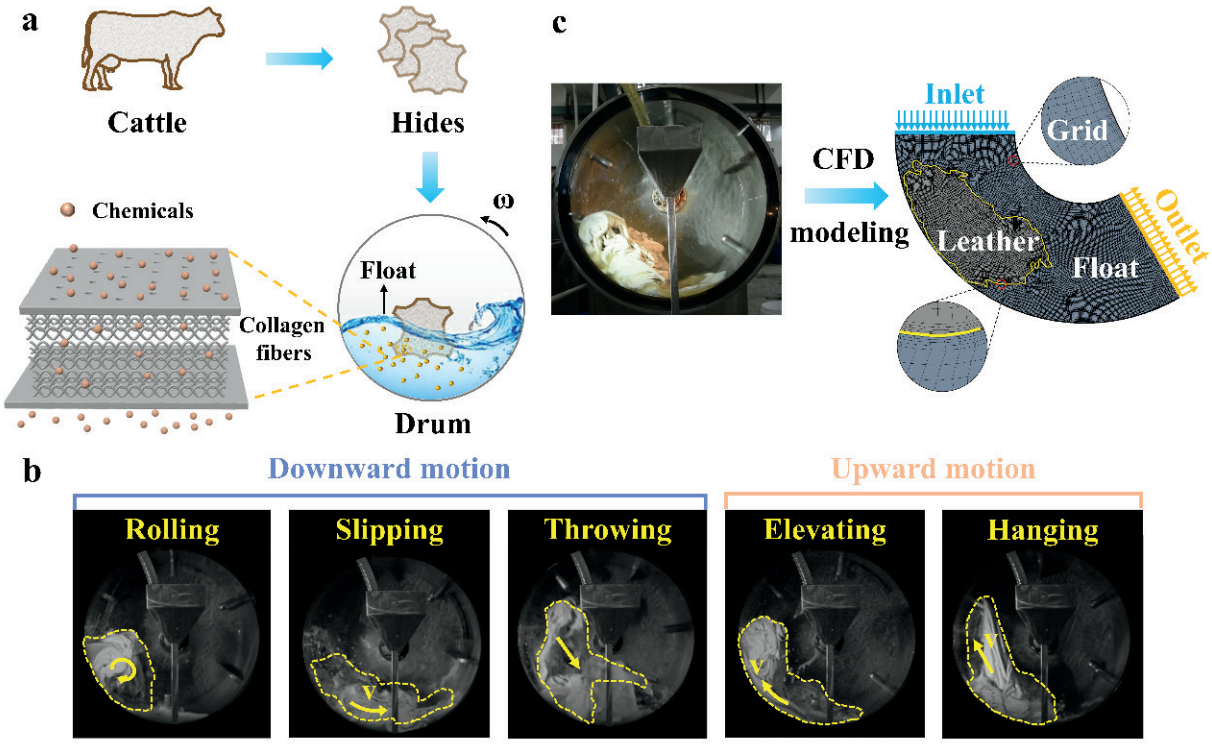

Figure 1. (a) Schematic of leather manufacturing. **(b)** Five typical motion states of leather in a rotating drum. **(c)** CFD modeling.

Experimental

Materials

Pickled cattle hides (pH 3.0, 1.5 mm thickness) and zirconium tanning agent of technical grade were provided by Sichuan Tingjiang New Material Co., Ltd. (Shifang, China). Analytical-grade magnesium oxide, nitric acid (65%–68% w/v aqueous solution) and hydrogen peroxide (30% w/v aqueous solution) were purchased from Chron Chemicals Co., Ltd. (Chengdu, China). The other chemicals used for leather processing were of technical grade.

Tanning experiments

Four pickled cattle hides were tanned with zirconium tanning agent to obtain leathers, as shown in Table I. Each pickled hide of approximately 10 kg was divided into four pieces (cut along directions parallel and perpendicular to the backbone) and used for a tanning trial. The drum rotation speed was individually set to 5, 10, 15, and 20 r/min. The motion characteristics of leather during tanning were analyzed by a visualization experiment system. The mass transfer behaviors of zirconium in leather were studied by measuring the change in the zirconium concentration of the tanning float and the zirconium content of leather. Tanning performance was evaluated by measuring the shrinkage temperatures and fiber dispersion of zirconium-tanned leathers.

Visualization of leather motions

The motion characteristics of leather were investigated by a visualization experiment system as shown in Figure 2. The drum rotation speed is in the range of 0–25 r/min, and the internal diameter and width of the drum were 800 and 400 mm, respectively. The front-end plate of the drum is transparent for easy observation of leather motions. Two baffles (90 mm width) and six cylindrical columns (30 mm diameter) are symmetrically arranged inside the drum. Three light sources were placed to reduce the negative impacts caused by uneven light distribution. A camera with 25 frames per second (fps) and a resolution of 1920×1080 pixels was placed 1200 mm away from the drum to capture the real-time position of the leather [Figure 2(c)]. The horizontal and vertical directions of the camera were calibrated by a laser leveler, where the lens was perpendicular to the image before shooting. A laptop was used to process the videos immediately to facilitate further data analysis. Adobe Premiere was used to edit the video [Figures 2(d) and 2(e)]. Image analysis was conducted using MATLAB to convert the original image into a binary image [Figure 2(f)], assigning 0 for drum areas (black) and 1 for the leather (white). The occurrence frequency and time percentage of each motion state of leather were counted.

As for the calculation of leather velocity, the shape center of leather was regarded as the centroid of leather, assuming a uniform density of leather. The instantaneous centroid coordinates of leather were extracted according to the binary image of each frame, the centroid displacement between two frames was measured, and the change of leather velocity within one frame (1/25 s) was ignored. The average velocity of leather in this frame was calculated and considered the instantaneous velocity of leather motion in this study.

Table I
Zirconium tanning process

Process	Material	Dosage (%)*	T (°C)	t (min)	Remarks
Pickling	Water	200	20		
	Sodium chloride	14		10	
	Pickled hide			20	Drain 40% float.
Tanning	Zirconium tanning agent	14	20	240	
Basifying	Magnesium oxide	2.2		180	
	Water	200	40	120	Still overnight. Next day, run 30 min.

*The percentages of materials were based on the weight of pickled cattle hide.

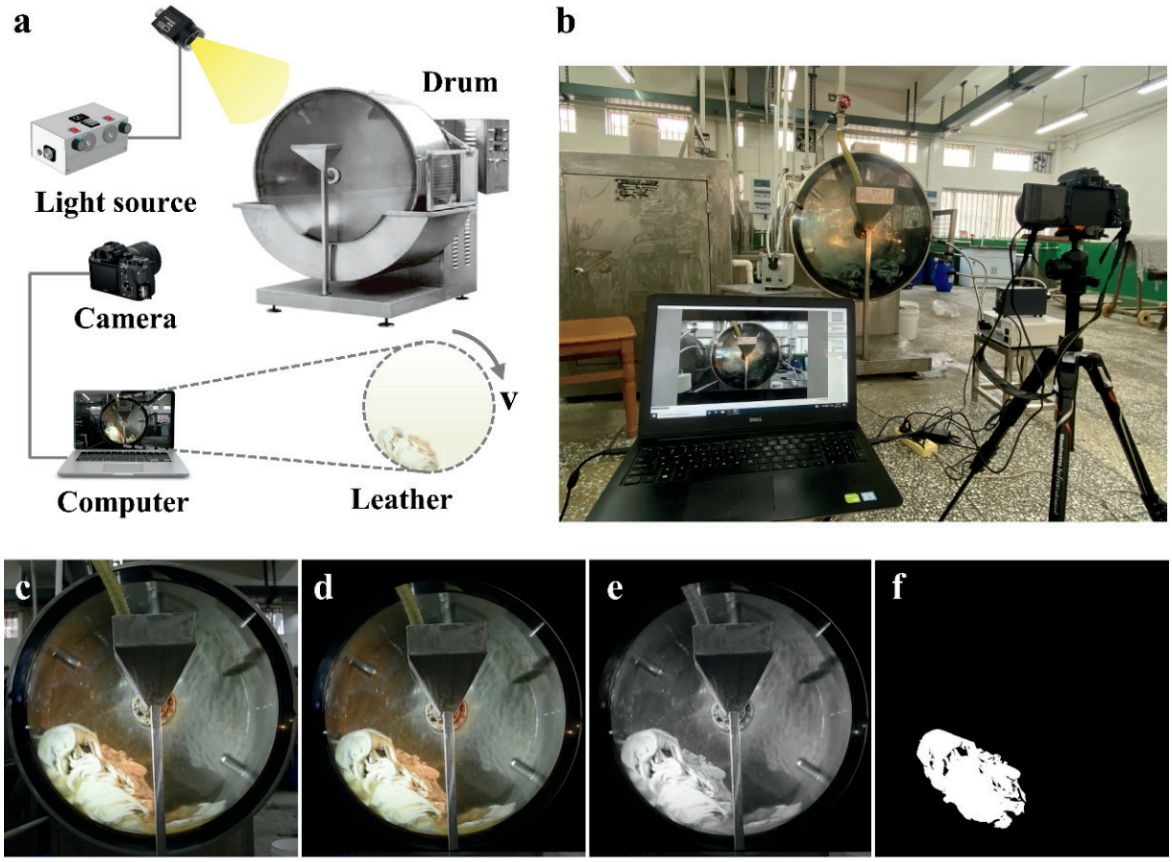

Figure 2. Visualization experiment: **(a)** Schematic of experiment system. **(b)** Photograph of the experimental system. **(c-f)** Processing of leather motion images: **(c)** shooting; **(d)** cutting; **(e)** gray processing; **(f)** binarizing.

Analysis of mass transfer of zirconium tanning agent in leather

Float samples were collected after tanning for 5, 10, 20, 30, 40, 60, 90, 120, 180 and 240 min. One mL of float sample was digested with 5 mL of nitric acid aqueous solution (65% *w*/*v*) and 1 mL of hydrogen peroxide aqueous solution (30% *w*/*v*) at 4 MPa and 200°C for 55 min in a microwave digestion instrument (Multiwave PRO, Anton Paar, Austria). The zirconium concentration of the digestion solution was determined by ICP-OES (Optima 2100DV, PerkinElmer, USA). The uptake of zirconium tanning agent by the leather was calculated with Equation (1):

$$\text{Zirconium uptake} = (C_0\text{-}C_t) / C_0 \times 100\% \quad (1)$$

where C_0 (mg/L) is the initial zirconium concentration of the tanning float, and C_t (mg/L) is the zirconium concentration of the float after tanning for t min.

Moreover, the leathers were sampled after tanning for 5, 30, 60, 90, 120, 180 and 240 min. The zirconium distribution in the leather was detected by EDS (INCA X-MAX 50, Oxford, UK). The leather samples were further split into three uniform layers, and each layer was dried to a constant weight at 102°C. Dried sample (0.5 g) was digested with 5 mL of nitric acid and 1 mL of hydrogen peroxide. The zirconium concentration of the digestion solution was measured by ICP-OES. The zirconium content of each layer was calculated using Equation (2):

$$\text{Zirconium content} = (c \times V) / w \times 100\% \quad (2)$$

where c is the zirconium concentration of the digestion solution (mg/L), V is the volume of the digestion solution (L), and w is the dry weight of the leather sample (mg).

Here, the total weight of the leather samples used for measuring the zirconium concentration was less than 50 g, viz. 0.5% of the total hide weight. Therefore, the hide weight loss affected the calculation of zirconium concentration slightly and was negligible.

The measurements were repeated thrice to obtain the average values and standard deviations.

Analysis of leather tanning performance

The leathers were horsed up for 24 h after tanning and sampled to determine the shrinkage temperature and porosity of zirconium-tanned leather. The shrinkage temperature was measured according to the standard method.[36] The porosity and morphology of the leather were analyzed by mercury intrusion porosimetry (MIP; AutoPore IV 9500, Micromeritics, USA) and scanning electron microscopy (SEM;

JSM-7500F, JEOL, Japan), respectively, using the leather samples lyophilized in a freeze dryer (LGJ-30F, XinYi, China).

CFD validation of leather motion states

Assumptions and governing equations

The following assumptions were performed to make the simulation results close to the actual situations and save computing time:

(i) The tanning float was assumed as an incompressible Newtonian fluid and the mixture of zirconium and water.

(ii) The tanning float was assumed as a turbulent and two-dimensional (2D) fluid and filled the whole computing region.

(iii) The physical properties of the fluid were the same with those of water.

(iv) The leather was considered as a 2D porous model with fluid inside.

The error resulting from the assumption for 2D modeling was caused by ignoring the leather deformation in the vertical direction of drum, and the error margin was ±27.4%.

Considering these assumptions, the governing equations for fluid flow are as follows.[37]

Continuity equation:

$$\frac{\partial u}{\partial x}+\frac{\partial v}{\partial y}=0 \tag{3}$$

where u and v are velocity components in x, y directions, m/s; x and y are coordinate directions, m.

Momentum equations:

$$\rho\left(u\frac{\partial u}{\partial x}+v\frac{\partial u}{\partial y}\right)=-\frac{\partial p}{\partial x}+\mu\left(\frac{\partial^2 u}{\partial x^2}+v\frac{\partial^2 u}{\partial y^2}\right) \tag{4}$$

$$\rho\left(u\frac{\partial v}{\partial x}+v\frac{\partial v}{\partial y}\right)=-\frac{\partial p}{\partial y}+\mu\left(\frac{\partial^2 v}{\partial x^2}+v\frac{\partial^2 v}{\partial y^2}\right) \tag{5}$$

where ρ is the density of fluid, kg/m^3; p is the operating pressure in the drum, Pa; μ is the dynamic viscosity of the fluid, kg/s.

Energy equation:

$$u\frac{\partial T}{\partial x}+v\frac{\partial T}{\partial y}=a\left(\frac{\partial^2 T}{\partial x^2}+\frac{\partial^2 T}{\partial y^2}\right) \tag{6}$$

where T is the temperature of fluid, K; a is the thermal diffusion coefficient, m^2/s

Concentration equation:

$$u\frac{\partial C}{\partial x}+v\frac{\partial C}{\partial y}=D_{AB}\left(\frac{\partial^2 C}{\partial x^2}+\frac{\partial^2 C}{\partial y^2}\right) \tag{7}$$

where C is the zirconium concentration in the fluid, kg/m^3; D_{AB} is the diffusion coefficient of zirconium in the fluid, m^2/s.

Boundary conditions

The boundary conditions are as follows:[38]

Fluid inlet: $u = u(t)$, $c = c_0$

Fluid outlet: $u = u(t)$

Leather surface: $u = 0$, $c = 0$

where $u(t)$ is the velocity of the fluid and set as a value based on the calculated results of the visualisation experiment, m/s. c_0 is the initial zirconium concentration in the fluid and calculated with equation (8), 3.4 mg/g.

$$c_0=\frac{P_1\times P_2\times M(\mathrm{Zr})}{P_3\times M(\mathrm{ZrO_2})} \tag{8}$$

where P_1 and P_3 are the mass percentages of the zirconium tanning agent and the float used in the tanning experiment, respectively; P_2 is the mass percentage of zirconium dioxide in the zirconium tanning agent; M(Zr) and M(ZrO_2) are the relative molecular masses of zirconium and zirconium dioxide, respectively.

Figure 3 shows the 2D geometric modelling for the tanning process. Based on the binarization image, the geometric feature of the leather

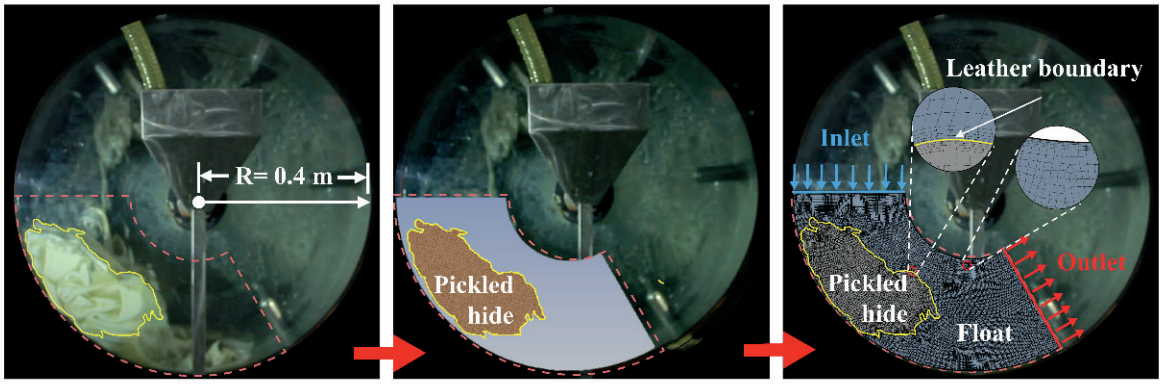

Figure 3. CFD modeling for tanning process (15 r/min).

was presented in the model. Auto CAD software was used to draw the outline of leather, and then the Ansys ICEM software was used to generate a quadrilateral mesh.

The velocity values of rolling, slipping, throwing, elevating and hanging motions were 0.23, 0.31, 0.35, 0.36 and 0.25 m/s, respectively. The mass transfer diffusion coefficient of zirconium was set as 2.88×10^{-5} m^2/s based on the evaluation method performed by Sathish.[39] Leather was defined as a porous medium whose porosity was set as 0.50 according to the MIP measurement results. The viscosity resistance coefficient and inertia resistance coefficient of leather were defined as the default values corresponding to 2.11×10^8 and 4.39, respectively.

Results and Discussion

Leather motion characteristics under different rotation speeds

During the tanning process, leathers shrink into ball shapes in the drum [Figure 2(c)] and represent motions with consecutive deformation [Figure 1(b)]. These irregular motions will lead to the ever-changing mass transfer behaviors of tanning agents. The aim of this work was to reveal the quantitative relationship between typical leather motions and the mass transfer of chemicals. Therefore, different leather motions were prepared by adjusting the drum rotating speed from 5 r/min to 20 r/min.

We previously found that five typical motion states of leather occur in the tanning process, where the rolling, slipping and throwing states were classified into downward motions, and the elevating and hanging states were classified into upward motions [Figure 1(b)].[30] In this study, the tanning images in one minute were captured using the visualization experiment system after the drum rotated stably, and the occurrence frequency and time percentage of each motion state of leather were counted. As shown in Figure 4(a), the duration of each motion state differs with increasing drum rotation speed. The rolling, slipping and elevating states of leather were the motion states that occurred most frequently in the tanning process, whose total duration was more than 80% of the tanning time. As the rotating speed increased from 5 r/min to 20 r/min, the durations of the rolling, slipping, throwing, and hanging states increased by 9.8%, 20.8%, 23.9%, and 59.7%, respectively; the duration of the elevating state decreased by 67.5%. No obvious differences in the height of elevating and throwing were observed under different rotation speeds of the drum. Figure 4(b) presents that the durations of upward and downward motions showed a logarithmic relationship with the drum rotation speed. In summary, leathers with different motion characteristics were obtained using different drum rotation speeds.

Mass transfer of zirconium tanning agent

Mass transfer of tanning agents is of great importance for tanning performance and leather properties.[40] In this section, the mass transfer of the zirconium tanning agent was evaluated by analyzing the adsorption kinetics of zirconium to leather and the distribution of zirconium in leather. The adsorption amounts of the zirconium tanning agent by leather increased over time and with increasing rotation speed [Figures 5(a)] and 5(b)]. The time for the adsorption equilibrium of zirconium under 15 and 20 r/min was approximately 120 min, whereas that under 5 and 10 r/min was approximately 180 min. The results suggested that the penetration process can be shorten by increasing drum rotation speed. The adsorption kinetics data were further fitted to pseudo-first-order (PFO) and pseudo-second-order (PSO) kinetic models. The PFO and PSO kinetic equations are as follows:[41,42]

$$\ln(q_e - q_t) = \ln q_e - k_1 t \tag{9}$$

$$\frac{t}{q_t} = \frac{1}{q_e} t + \frac{1}{k_2 q_e^2} \tag{10}$$

where q_t and q_e are the amounts of zirconium adsorbed (mg/g) at t min and equilibrium, respectively, and k_1 and k_2 are the PFO rate constants (min^{-1}) and the PSO rate constants (g/[mg·min]), respectively.

The PFO and PSO kinetic parameters for zirconium adsorption during the tanning process are listed in Table II. The correlation

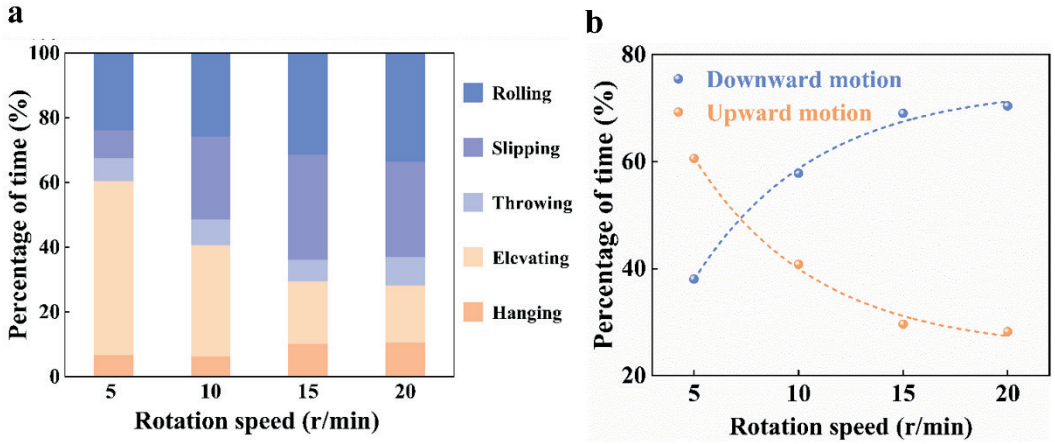

Figure 4. Motion characteristics of leather in the tanning process under different drum rotation speeds: **(a)** Percentage of duration of each motion state of leather during tanning process. **(b)** Fitting curves showing the relationship between the durations of upward and downward motions of leather and the drum rotation speed during tanning process.

Table II

PSO and PFO kinetic parameters for zirconium adsorption

Group	$q_e exp$ (mg/g)	PFO kinetic model				PSO kinetic model			
		k_1 (min^{-1})	R^2	$q_e cal$ (mg/g)	Error (%)	k_2 (g/(mg·min)$^{-1}$)	R^2	$q_e cal$ (mg/g)	Error (%)
5 r/min	30.76	5.03×10^{-2}	0.6925	28.83	6.27	3.15×10^{-4}	0.9963	31.50	-2.41
10 r/min	42.36	3.64×10^{-2}	0.7738	40.07	5.41	2.59×10^{-3}	0.9962	43.18	-1.94
15 r/min	48.71	5.62×10^{-2}	0.7984	47.29	2.92	2.90×10^{-3}	0.9994	49.95	-2.55
20 r/min	48.15	5.80×10^{-2}	0.6252	45.79	1.79	2.75×10^{-3}	0.9983	49.65	-3.11

$q_e exp$: determined by experiments.

$q_e cal$: calculated by the PFO or PSO kinetic models.

$Error\ (\%) = (q_e exp - q_e cal)/q_e exp \times 100$.

R^2: correlation coefficient.

coefficients (R^2) obtained by the PSO kinetic model were all higher than 0.99, whereas those obtained by the PFO kinetic model were lower than 0.80. The results indicated that the zirconium adsorption processes followed the PSO kinetics [Figure 5(c)]. Moreover, the higher k_2 values for tanning under 15 and 20 r/min than those under 5 and 10 r/min indicated that high rotation speed resulted in the rapid adsorption of zirconium. The data in Figure 5(d) shows the amounts of zirconium absorbed by each layer of leather under different rotation speeds. The amounts of zirconium absorbed by the middle layer were lower than those absorbed by the grain and flesh layers under 5 and 10 r/min, and the amounts of zirconium absorbed by the middle layer were close to those absorbed by grain and flesh layers under 15 and 20 r/min. The results indicated that the zirconium was distributed more evenly in the tanned leather under higher rotation speed. In summary, tanning under high rotation speed achieved better mass transfer than tanning under low rotation speed. In addition, no apparent differences in the adsorption amounts and rates of zirconium were observed between 15 and 20 r/min, which suggested that the transfer and uptake of zirconium could not be further improved by increasing the rotation speed above 15 r/min.

The tanning performance of leather was evaluated by analyzing the shrinkage temperature (for characterizing hydrothermal stability) and fiber dispersion of leather. The high shrinkage temperature and fiber dispersion degree of leather represent excellent tanning performance. As shown in Figure 5(e), the shrinkage temperature of leather gradually increases as the rotating speed increased from 5/min to 15 r/min. SEM images of the leather cross-sections showed that the leather collagen fibers tanned under high rotation speed were highly dispersed [Figure 5(f)]. Overall, leather tanned under high rotation speed exhibited excellent tanning performance, because high rotation speed resulted in rapid zirconium penetration, uniform zirconium distribution and high zirconium uptake. The tanning performance under 15 and 20 r/min were similar, which may be explained by the fact that the penetration, distribution and uptake of zirconium under 15 r/min were close to those under 20 r/min.

Effect of leather motion states on mass transfer analyzed by CFD

Leather is a fibrous material that has multiple hierarchical structures and unevenly distributed pores [Figure 5(f)]. Pores in the leather matrix always deform during the tanning process, which makes a connection between the leather and float in the drum. The connection presents diverse and transient features, resulting in the varying mass transfer of zirconium at different moments. The data in Figures 4 and 5 demonstrate that different rotation speeds lead to different leather motions and mass transfer rates of zirconium. As the rotation speed increased, the durations of the rolling and slipping states increased, and the mass transfer of zirconium and leather tanning performance were improved. The results implied that leather motion has a strong connection with the mass transfer of tanning agent, and the rolling and slipping states should be conducive to the mass transfer. In this section, the CFD method was therefore used to further analyze the flow field of the float and the mass transfer of zirconium under typical leather motion states to clarify the effects of leather motion states on the mass transfer.

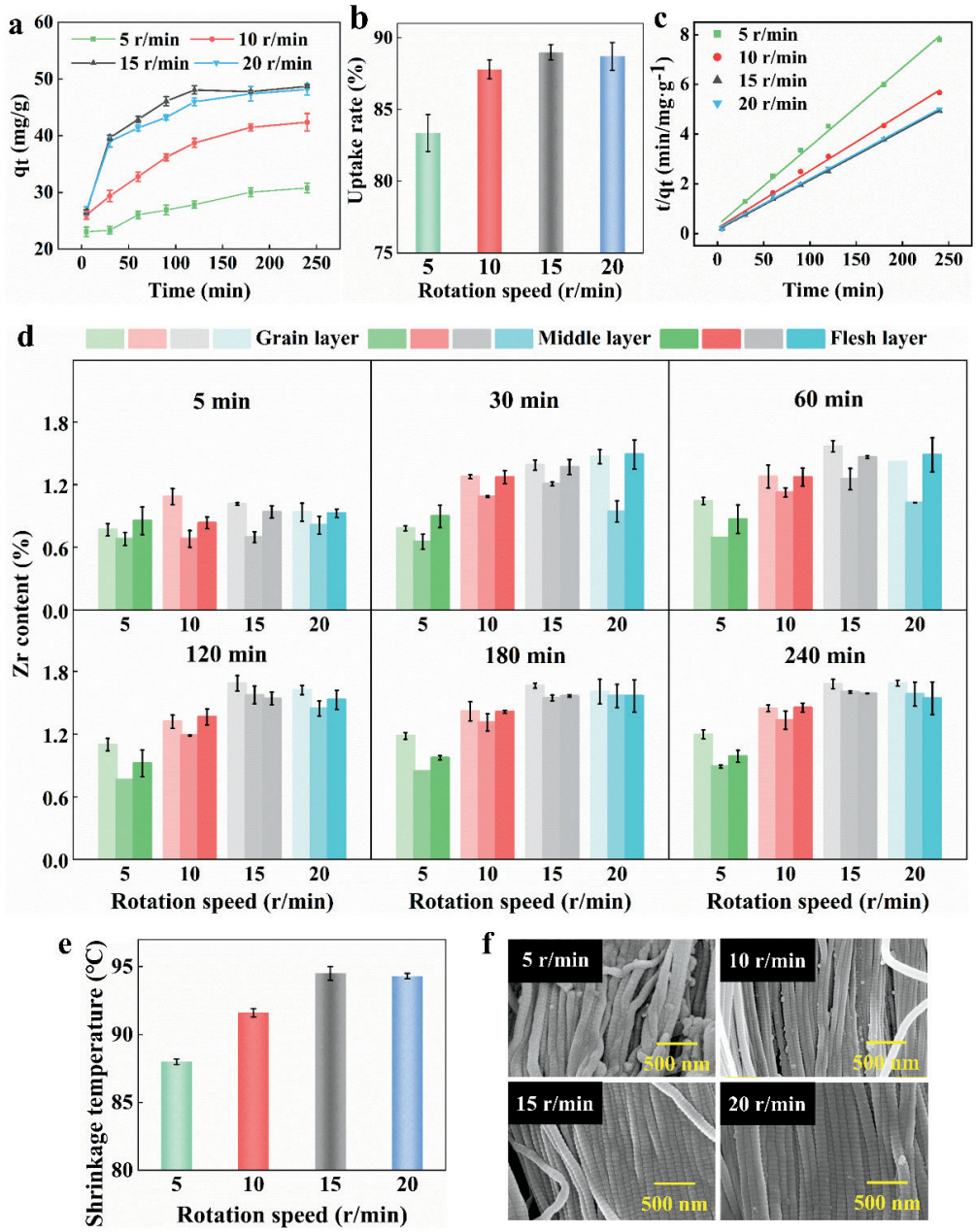

Figure 5. Adsorption kinetics and tanning performance of tanning agent under different rotation speeds. **(a)** Adsorption amount of zirconium by leather over time. **(b)** Uptake rate of zirconium tanning agent. **(c)** Fitting of zirconium adsorption data to the PSO kinetic model. **(d)** Zirconium distribution in grain, middle and flesh layers of leather. **(e)** Shrinkage temperature of leather. **(f)** SEM images of the cross-sections of leathers.

Velocity distribution

Figure 6 shows the instantaneous flow field of the float under five typical leather motion states. The maximum velocity of the float was 1.92 m/s during leather throwing, which was 2.56 times of that during leather hanging. This result indicates that the motion states of leather have a great influence on the flow field. The maximum velocity of the float was higher than 1.5 m/s when the leather was under slipping, throwing and rolling motions (downward motions), whereas the maximum velocity of the float was less than 1 m/s when the leather is elevating and hanging (upward motions). This outcome may be due to the downward motions of leather propelling the flow of the float. The float velocity near the rolling leather surface was the highest, which may be attributed to the strong scouring action of the float on the rolling leather surface. The rolling motion contributed the most to rapid float flow, which implies that the rolling motion should be most beneficial to the mass transfer of tanning agent.

Mass transfer of zirconium

Mass transfer analysis was conducted based on the data in steady-state, where the amounts of zirconium in the leather and float were at equilibrium and the mass transfer was suspended. The mass

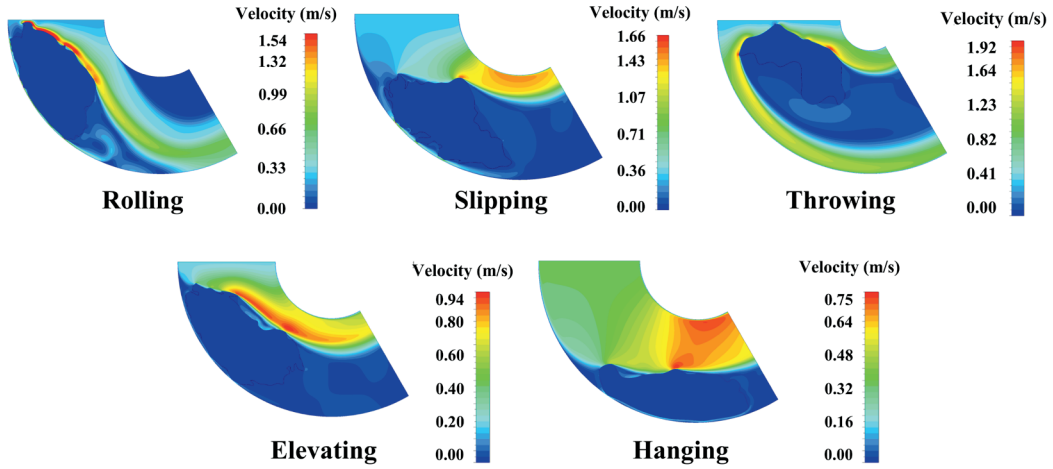

Figure 6. Flow field under five typical leather motion states.

fractions of zirconium in the float when the leather was under five typical motion states are shown in Figure 7. The zirconium concentration gradients near the leather surface were higher during leather throwing and rolling, compared with during leather slipping and hanging. The results means that the rolling and throwing of leather are more conducive to the mass transfer of zirconium than the other three motion states.

The simulated mass transfer rates of zirconium under the different leather motion states were calculated by Fick's law:

$$M_r = \frac{D_{AB}}{L_W} \int_0^{L_w} \left. \frac{\partial C}{\partial Y} \right|_{Y=0} dl \tag{11}$$

where M_r *is* the simulated mass transfer rate of zirconium, mg/(m²·s); D_{AB} is the diffusion coefficient of zirconium in the float, m²/s; L_W is the length of the leather boundary, m; C is the zirconium concentration in the float, kg/m³; dl is the microelement of leather boundary, m; Y is the penetration depth of zirconium in leather, m.

Considering that the zirconium mass transfer rate at a specific moment in the experiment is difficult to obtain, the given data are the averaged values calculated using Eq. (12):

$$\overline{M_r} = \frac{M_{Zr} \bullet \rho_H \bullet L_H}{m_H t_M} \tag{12}$$

where $\overline{M_r}$ is the average value of the mass transfer rate of zirconium in the experiment, mg/(m²·s); M_{Zr} is the mass of zirconium absorbed by the leather at the end of the tanning process, mg; ρ_H is the density of the pickled hide, 1.432 kg/m³; L_H is the thickness of the pickled hide, m; m_H is the mass of the pickled hide, kg; t_M is the time for the adsorption equilibrium of zirconium, s.

The simulated zirconium mass transfer rates were compared with the experimental data (Figure 8). The mass transfer rates of zirconium during leather throwing and rolling were obviously higher than those during the other three motions. This result indicates that leather's throwing and rolling motions play important roles in the mass transfer. Increasing the duration of the throwing and rolling

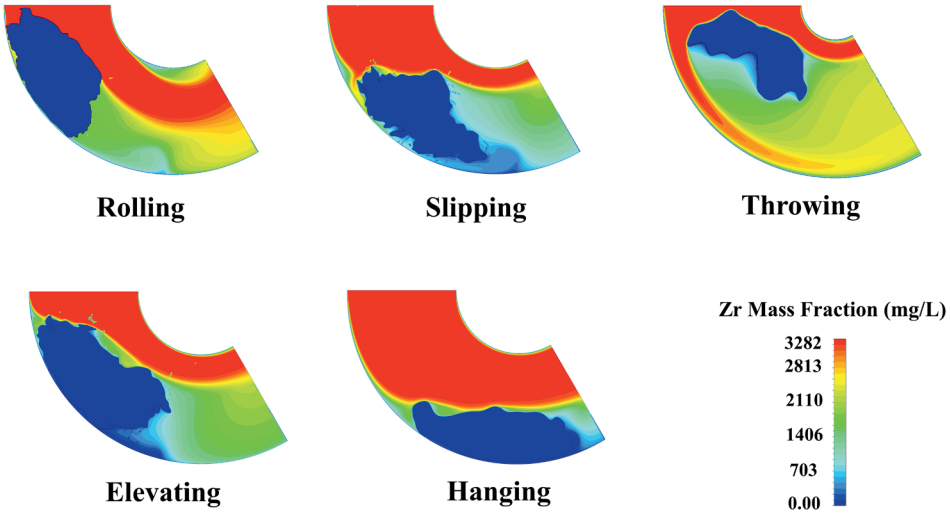

Figure 7. Mass fractions of zirconium under five typical leather motion states.

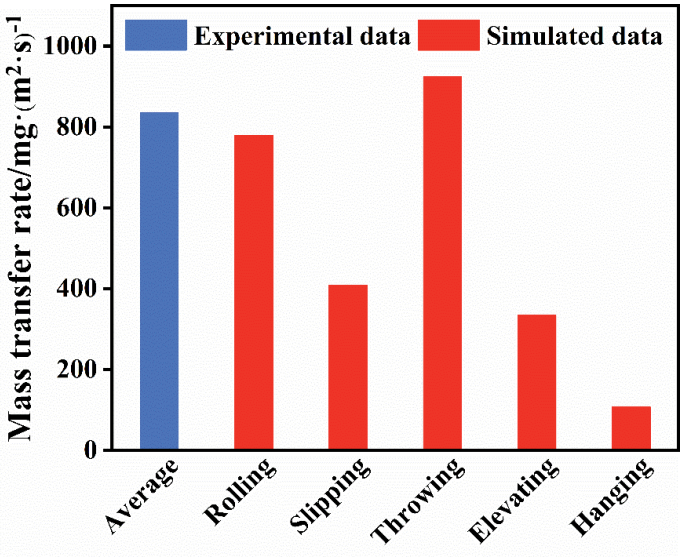

Figure 8. Comparison between experimental and simulated results (15 r/min).

states in leather production is beneficial to enhancing mass transfer and shortening tanning time. The average values of zirconium mass transfer rates in the experiment were nearly 1.5 times of the simulated values (15 r/min), which may be caused by the rapid suction and ejection of the float within leather pores. Future work will further elucidate how the porous structure of leather affects the mass transfer of chemicals. Notably, the loading rate of drum greatly affects the motions of leather and the mass transfer of chemicals. The applicability of this model at a high loading rate of drum needs to be further verified.

Conclusion

Leather motion states were closely related to the mass transfer and distribution of tanning agent in leather and the tanning performance of leather. Rolling motion was beneficial for the rapid penetration and uniform distribution of tanning agent, whereas hanging motion had the opposite effect. Rapid penetration leads to high-efficiency production and uniform distribution of tanning agent leads to excellent tanning performance. The results indicate that greater tanning performance can be achieved by increasing rolling motion and decreasing hanging motion. This work proposes a clear direction to regulate mechanical actions, which is useful for designing operating conditions or novel equipment for high-quality leather production.

Acknowledgement

This work was supported by Natural Science Foundation of Sichuan Province (2022NSFSC1180) and Research Institutes of Leather and Footwear Industry of Wenzhou (20H1061).

References

1. Dixit, S., Yadav, A., Dwivedi, P.D., Das, M.; Toxic hazards of leather industry and technologies to combat threat: a review. *J. Clean. Prod.* **87**, 39-49, 2015.
2. Saravanabhavan, S., Thanikaivelan, P., Rao, J.R., Nair, B.U., Ramasami, T.; Reversing the conventional leather processing sequence for cleaner leather production. *Environ. Sci. Technol.* **40(3)**, 1069-1075, 2006.
3. Covington, A. D.; Tanning Chemistry: The Science of Leather, Royal Society of Chemistry, Cambridge, 195-201, 2009.
4. Hansen, É., de Aquim, P.M., Hansen, A.W., Cardoso, J.K., Ziulkoski, A.L., Gutterres, M.; Impact of post-tanning chemicals on the pollution load of tannery wastewater. *J. Environ. Manag.* **269**, 110787, 2020.
5. Garcia, N.G., dos Reis, E.A.P., Budemberg, E.R., Agostini, D.L.D.S., Salmazo, L.O., Cabrera, F.C., Job, A.E.; Natural rubber/leather waste composite foam: A new eco-friendly material and recycling approach. *J. Appl. Polym. Sci.* **132(11)**, 2015.
6. He, X., Ding, W., Yu, Y., Zhou, J. F., Shi, B.; Insight into the correlations between fiber dispersion and physical properties of chrome tanned leather. *JALCA* **115(1)**, 23-29, 2020.
7. Sun, S., Wang, X., Zhu, X., Liu, X., Guo, P., Tian, Y.; Synthesis of an amphiphilic amphoteric peptide-based polymer for organic chrome-free ecological tanning. *J. Clean. Prod.* **330**, 129880, 2022.
8. Mao, Q., Yang, Q. J., Liu, Y., Cao, W.; Experimental and numerical study of droplet formation with Marangoni instability. *Chem. Eng. Sci.* **268**, 118369, 2023. Zheng et al., 2014
9. Yao, Y.; Enhancement of mass transfer by ultrasound: Application to adsorbent regeneration and food drying/dehydration. *Ultrason. Sonochem.* **31**, 512-531, 2016.
10. Wegener, M., Paschedag, A.R. and Kraume, M.; Mass transfer enhancement through Marangoni instabilities during single drop formation. *Int. J. Heat. Mass. Tran.* **52(11-12)**, 2673-2677, 2009.
11. Ahmed, S.M., Phan, A.N., Harvey, A.P.; Mass transfer enhancement as a function of oscillatory baffled reactor design. *Chem. Eng. Process.* **130**, 229-239, 2018.
12. Dehghannya, J., Pourahmad, M., Ghanbarzadeh, B., Ghaffari, H.; Heat and mass transfer enhancement during foam-mat drying process of lime juice: Impact of convective hot air temperature. *Int. J. Therm. Sci.* **135**, 30-43, 2019.
13. Fishwick, R. P., Winterbottom, J. M., Stitt, E. H.; Effect of gassing rate on solid–liquid mass transfer coefficients and particle slip velocities in stirred tank reactors. *Chem. Eng. Sci.* **58(3-6)**, 1087-1093, 2003.
14. Mohammed, I., Bauer, T., Schubert, M., Lange, R.; Liquid–solid mass transfer in a tubular reactor with solid foam packings. *Chem. Eng. Sci.* **108**, 223-232, 2014.
15. Wang, Y.N., Hu, L.; Essential role of isoelectric point of skin/leather in leather processing. *J. Leather Sci. Eng.* **4(1)**, 25, 2022.
16. Yang, T. Q., Zeng, Y. H., Sun, Q. Y., Lei, C., Shi, B.; Effect of pickling materials on leather quality from a hide surface charge perspective. *JALCA* **117(7)**, 279-87, 2022.

17. Wang, Y.N., Huang, W. L., Zhang, H., Tian, L., Zhou, J. F., Shi, B.; Surface charge and isoelectric point of leather: a novel determination method and its application in leather making. *JALCA* **112(07)**, 224-231, 2017.
18. Yu, Y., Wang, Y.N., Ding, W., Zhou, J. F., Shi, B.; Preparation of highly-oxidized starch using hydrogen peroxide and its application as a novel ligand for zirconium tanning of leather. *Carbohyd. Polym.* **174**, 823-829, 2017.
19. Ma, J., Gao, J., Wang, H., Lyu, B., Gao, D.; Dissymmetry gemini sulfosuccinate surfactant from vegetable oil: A kind of environmentally friendly fatliquoring agent in the leather industry. *ACS Sustain. Chem. Eng.* **5(11)**, 10693-10701, 2017.
20. Ma, J.Z., Liu, Q., Wu, M., Tian, Z.; Preparation and assistant-dyeing of formaldehyde-free amphoteric acrylic retanning agent. *J. Leather Sci. Eng.* **3**, 1-13, 2021.
21. Wang, X., Lan, X., Zhu, X., Sun, S.; Preparation of a ricinolein acid modified amphoteric polyurethane for leather cleaner and simplifying production. *J. Clean. Prod.* **330**, 129877, 2022.
22. Ariram, N., Sathish, M., Madhan, B.; Chemical/water-free deliming process using supercritical carbon dioxide: a step toward greener leather manufacture. *ACS Sustain. Chem. Eng.* **8(31)**, 11747-11754, 2020.
23. Sathish, M., Silambarasan, S., Madhan, B., Rao, J.R.; Exploration of GSK'S solvent selection guide in leather industry: a CSIR-CLRI tool for sustainable leather manufacturing. *Green. Chem.* **18(21)**, 5806-5813, 2016.
24. Kanagaraj, J., Panda, R.C., Senthilvelan, T., Gupta, S.; Cleaner approach in leather dyeing using graft copolymer as high performance auxiliary: related kinetics and mechanism. *J. Clean. Prod.* **112**, 4863-4878, 2016.
25. Wang, Z., Wang, Y.N., Yu, Y., Shi, B.; Tanning performance of a novel chrome-free complex tanning agent: penetration and distribution. *JALCA* **116(8)**, 277-283, 2021.
26. Ding, W.; Bridging-induced densification strategy based on biomass-derived aldehyde tanning integrated with terminal Al (III) crosslinking towards high-performance chrome-free leather production. *J. Environ. Manage.* **307**, 114554, 2022.
27. Santos, D.A., Petri, I.J., Duarte, C.R., Barrozo, M.A.S.; Experimental and CFD study of the hydrodynamic behavior in a rotating drum. *Powder. Technol.* **250**, 52-62, 2013.
28. Shi, X., Xiang, Y., Wen, L.X., Chen, J.F.; CFD analysis of liquid phase flow in a rotating packed bed reactor. *Chem. Eng. J.* **228**, 1040-1049, 2013.
29. Tang, X., Yue, Y., Wang, S., Shen, Y.; Modelling of gas-solid-liquid flow and particle mixing in a rotary drum. *Powder. Technol.* **409**, 117758, 2022.
30. Jiang, Z.C., Lin, Y.R., Xie, G., Zeng, Y.H., Wang, Y.N.; Motion characteristics of leather in drum and influence on mass transfer for chemicals. *Chemical Engineering (China).* **50(8)**, 26-30, 2022.
31. Tang, Y. L., Zhao, J. T., Zhou, J. F., Zeng, Y. H., Zhang, W. H. and Shi, B.; Highly efficient removal of Cr (III)-poly (acrylic acid) complex by coprecipitation with polyvalent metal ions: Performance, mechanism, and validation. *Water Res.* **178**, 115807, 2020.
32. Li, Y. C., Guo, R. J., Lu, W. H. and Zhu, D. Y.; Research progress on resource utilization of leather solid waste. *Journal of Leather Science and Engineering* **1**, 1-17, 2019.
33. Yu, Y., Lin, Y. R., Zeng, Y. H., Wang, Y. N., Zhang, W. H., Zhou, J. F. and Shi, B.; Life cycle assessment for chrome tanning, chrome-free metal tanning, and metal-free tanning systems. *ACS Sustainable Chem. Eng.* **9(19)**, 6720-6731, 2021.
34. Yu, Y., Wang, H., Wang, Y., Zhou, J. F. and Shi, B.; Construction of a chrome-free tanning system based on highly-oxidized starch–zirconium complexes. *JALCA* **117(3)**, 87-95, 2022.
35. Yu, Y., Wang, H., Wang, Y.N., Zhou, J. F. and Shi, B.; Chrome-free synergistic tanning system based on biomass-derived hydroxycarboxylic acid–zirconium complexes. *J. Clean. Prod.* **336**, 130428, 2022.
36. IUP 16; Measurement of shrinkage temperature up to 100°C. *J. Soc. Leath. Tech. Ch.* **84**, 359–362, 2000.
37. Wang, X., Wang, Y., Chen, H., Zhu, Y.; A combined CFD/visualization investigation of heat transfer behaviors during geyser boiling in two-phase closed thermosyphon. *Int. J. Heat. Mass. Tran.* **121**, 703-714, 2018.
38. Talukdar, P., Iskra, C.R., Simonson, C.J.; Combined heat and mass transfer for laminar flow of moist air in a 3D rectangular duct: CFD simulation and validation with experimental data. *Int. J. Heat. Mass. Tran.* **51(11-12)**, 3091-3102, 2008.
39. Sathish, M., Dhathathreyan, A., Rao, J.R.; Ultraefficient tanning process: role of mass transfer efficiency and sorption kinetics of Cr (III) in leather processing. *ACS Sustain. Chem. Eng.* **7(4)**, 3875-3882, 2019.
40. Gao, D., Wang, P., Shi, J., Li, F., Li, W., Lyu, B., Ma, J.; A green chemistry approach to leather tanning process: cage-like octa (amino-silsesquioxane) combined with Tetrakis (hydroxymethyl) phosphonium sulfate. *J. Clean. Prod.* **229**, 1102-1111, 2019.
41. Ho, Y.S., McKay, G.; Pseudo-second order model for sorption processes. *Process. Biochem.* **34(5)**, 451-465, 1999.
42. Haerifar, M., Azizian, S.; An exponential kinetic model for adsorption at solid/solution interface. *Chem. Eng. J.* **215**, 65-71, 2013.